Emerald Insight

Engineering Computations

Factorized high dimensional model representation for structural reliability analysis
B.N. Rao Rajib Chowdhury

Article information:

For Authors

If you would like to write for this, or any other Emerald publication, then please use our Emerald for Authors service information about how to choose which publication to write for and submission guidelines are available for all. Please visit www.emeraldinsight.com/authors for more information.

About Emerald www.emeraldinsight.com

Emerald is a global publisher linking research and practice to the benefit of society. The company manages a portfolio of more than 290 journals and over 2,350 books and book series volumes, as well as providing an extensive range of online products and additional customer resources and services.

Emerald is both COUNTER 4 and TRANSFER compliant. The organization is a partner of the Committee on Publication Ethics (COPE) and also works with Portico and the LOCKSS initiative for digital archive preservation.

*Related content and download information correct at time of download.

Factorized high dimensional model representation for structural reliability analysis

B.N. Rao and Rajib Chowdhury

*Structural Engineering Division, Department of Civil Engineering,
Indian Institute of Technology Madras, Chennai, India*

Abstract

Purpose – To develop a new computational tool for predicting failure probability of structural/mechanical systems subject to random loads, material properties, and geometry.

Design/methodology/approach – High dimensional model representation (HDMR) is a general set of quantitative model assessment and analysis tools for capturing the high-dimensional relationships between sets of input and output model variables. It is a very efficient formulation of the system response, if higher order variable correlations are weak and if the response function is dominantly of additive nature, allowing the physical model to be captured by the first few lower order terms. But, if multiplicative nature of the response function is dominant then all right hand side components of HDMR must be used to be able to obtain the best result. However, if HDMR requires all components, which means 2^N number of components, to get a desired accuracy, making the method very expensive in practice, then factorized HDMR (FHDMR) can be used. The component functions of FHDMR are determined by using the component functions of HDMR. This paper presents the formulation of FHDMR approximation of a multivariate limit state/performance function, which is dominantly of multiplicative nature. Given that conventional methods for reliability analysis are very computationally demanding, when applied in conjunction with complex finite element models. This study aims to assess how accurately and efficiently HDMR/FHDMR based approximation techniques can capture complex model output uncertainty. As a part of this effort, the efficacy of HDMR, which is recently applied to reliability analysis, is also demonstrated. Response surface is constructed using moving least squares interpolation formula by including constant, first-order and second-order terms of HDMR and FHDMR. Once the response surface form is defined, the failure probability can be obtained by statistical simulation.

Findings – Results of five numerical examples involving structural/solid-mechanics/geo-technical engineering problems indicate that the failure probability obtained using FHDMR approximation for the limit state/performance function of dominantly multiplicative in nature, provides significant accuracy when compared with the conventional Monte Carlo method, while requiring fewer original model simulations.

Originality/value – This is the first time where application of FHDMR concepts is explored in the field of reliability and system safety. Present computational approach is valuable to the practical modeling and design community, where user often suffers from the curse of dimensionality.

Keywords Failure (mechanical), Modelling

Paper type Research paper

Introduction

The basic purpose of structural reliability analysis is the evaluation of failure probability referenced to a given limit state/performance function $g(x)$. In reality,

the inherent difficulties in reliability estimation arise due to implicit nature and high nonlinearity of $g(x)$. Therefore, a detailed finite element (FE) modeling of the structure is necessary in combination with reliability analysis tools. FE methods for linear and nonlinear structures in conjunction with first- or second-order reliability method (FORM/SORM) (Rackwitz, 2001; Ditlevsen and Madsen, 1996; Madsen *et al.*, 1986; Breitung, 1984) have been successfully applied for structural reliability computations (Liu and Der Kiureghian, 1991). FORM/SORM is based on linear (FORM) or quadratic approximation (SORM) of the limit state/performance function at a most probable point (MPP). Experience has shown that FORM/SORM solutions provide significant accuracy for engineering purposes, provided that the MPP is accurately found, the limit state/performance function at MPP is close to being linear or quadratic, and no multiple MPPs exist. The MPP can be located by various gradient-based optimization algorithms, which in turn require first- and/or second-order response sensitivities or gradients. If these gradients can be found analytically, FORM/SORM is quite efficient. Otherwise, FORM/SORM can be ineffective, for instance, when response sensitivities are not available or when sensitivity analysis is computationally intensive. A prime example is the merging of FORM/SORM with commercial FE programs, where multiple analysis codes from third-party sources are frequently employed without any knowledge of gradients. In that case, FORM/SORM may yield inaccurate reliability solutions or create computationally inefficient results when using gradients from finite-difference approximations. Furthermore, for highly nonlinear performance functions, which exist in many structural problems, results based on FORM/SORM must be interpreted with caution. If the Rosenblatt or Nataf transformation are used to map non-Gaussian random input into its standard Gaussian space then, the limit state/performance function becomes highly nonlinear. In this case, FORM/SORM produces inadequate reliability estimates (Bjerager, 1988). Furthermore, the existence of multiple MPPs could give rise to large errors in standard FORM/SORM approximations (Ditlevsen and Madsen, 1996; Der Kiureghian and Dakessian, 1998). In that case, multi-point FORM/SORM along with the system reliability concept is required for improving component reliability analysis (Der Kiureghian and Dakessian, 1998).

In these cases, simulation methods (Schuëller *et al.*, 2004; Au and Beck, 2001; Melchers, 1989; Bjerager, 1988; Rubinstein, 1981) seem to be a suitable alternative. But the main disadvantage is that, simulation methods require tremendous computational effort due to large number of deterministic structural analysis for different realizations of the random variables. Several issues related to the applicability of FORM/SORM and the efficiency of simulation methods for reliability analysis have lead many researchers to assess and improve the viability of alternate approximate methods in the field of reliability and system safety.

This paper explores the potential of a new class of computational methods, referred to as High Dimensional Model Representation (HDMR) (Sobol, 2003; Li *et al.*, 2001a, b, 2002; Alis and Rabitz, 2001; Rabitz *et al.*, 1999; Rabitz and Alis, 1999; Wang *et al.*, 1999) and factorized HDMR (FHDMR) (Tunga and Demiralp, 2004, 2005), for predicting reliability of structural/mechanical systems subject to random loads, material properties, and geometry. The idea of HDMR for multivariate function approximation, originally adopted for piece wise continuous function (Chowdhury *et al.*, 2007), has been extended for reliability analysis (Chowdhury *et al.*, 2008). Primary focus of this paper is to conduct a comparative assessment of HDMR and FHDMR for failure

probability estimation. The paper is organized as follows. Section 2 presents a brief overview of HDMR. Section 3 presents the formulation of FHDMR. Section 4 presents response surface generation using FHDMR. Section 5 details the simulation method for evaluation of reliability using the response surface generated by HDMR and FHDMR. Section 6 presents five numerical examples to illustrate the performance of the present methods. Comparisons have been made with direct Monte Carlo simulation (MCS) method to evaluate the accuracy and the computational efficiency of the present methods.

Fundamentals of HDMR

In recent years there have been efforts to develop efficient methods to approximate multivariate functions in such a way that the component functions of the approximation are ordered starting from a constant and gradually approaching to multivariance as we proceed along the terms like first-order, second-order and so on. One such method is HDMR (Sobol, 2003; Li *et al.*, 2001a, b, 2002; Alis and Rabitz, 2001; Rabitz *et al.*, 1999; Rabitz and Alis, 1999; Wang *et al.*, 1999). HDMR is a general set of quantitative model assessment and analysis tools for capturing the high-dimensional relationships between sets of input and output model variables. It is a very efficient formulation of the system response, if higher-order variable correlations are weak, allowing the physical model to be captured by the first few lower-order terms. Practically for most well-defined physical systems, only relatively low order correlations of the input variables are expected to have a significant effect on the overall response (Sobol, 2003; Li *et al.*, 2001a, b, 2002; Alis and Rabitz, 2001; Rabitz *et al.*, 1999; Rabitz and Alis, 1999; Wang *et al.*, 1999). HDMR expansion utilizes this property to present an accurate hierarchical representation of the physical system. The notion of "high" dimensionality is system-dependent, with some situations being considered high for practical reasons at $N \sim 3$–5, while others will only reach that level of complexity for $N > 10$ or more.

Let the N(dimensional vector $\mathbf{x} = \{x_1, x_2, \ldots, x_N\}$, represent the input random variables of the computational model under consideration, and the limit state as $g(x)$. Since the influence of the input variables on the limit state can be independent and/or cooperative, HDMR expresses the limit state $g(x)$ as a hierarchical correlated function expansion in terms of the input random variables as:

$$
g(x) = g_0 + \sum_{i=1}^{N} g_i(x_i) + \sum_{1 \leq i_1 < i_2 \leq N} g_{i_1 i_2}(x_{i_1}, x_{i_2}) + \cdots + \sum_{1 \leq i_1 < \cdots < i_l \leq N} g_{i_1 i_2 \ldots i_l}(x_{i_1}, x_{i_2}, \ldots, x_{i_l})
$$
$$
+ \cdots + g_{12 \ldots N}(x_1, x_2, \ldots, x_N),
$$
(1)

where g_0 is a constant term representing the zeroth-order component function or the mean response of $g(x)$. The function $g_i(x_i)$ is a first-order term expressing the effect of variable x_i acting alone, although generally nonlinearly, upon the output $g(x)$. The function $g_{i_1 i_2}(x_{i_1}, x_{i_2})$ is a second-order term, which describes the cooperative effects of the variables x_{i_1} and x_{i_2} upon the output $g(x)$. The higher order terms gives the cooperative effects of increasing numbers of input variables acting together to influence the output $g(x)$. The last term $g_{12 \ldots N}(x_1, x_2, \ldots, x_N)$ contains any residual dependence of all the input variables locked together in a cooperative way to influence

the output $g(x)$. If there is no cooperation between the input variables, then only zeroth-order and first-order terms will appear in the expansion. Once all the relevant component functions in equation (1) are determined and suitably represented, then the component functions constitute HDMR, thereby replacing the original computationally expensive method of calculating $g(x)$ by the computationally efficient model. Usually the higher order terms in equation (1) are negligible (Alis and Rabitz, 2001; Li *et al.*, 2001a, b; Rabitz *et al.*, 1999; Rabitz and Alis, 1999) such that HDMR with only low order correlations to second-order, amongst the input variables are typically adequate in describing the output behavior (Li *et al.*, 2001b; Rabitz *et al.*, 1999; Rabitz and Alis, 1999) and this has been verified in a number of computational studies (Wang *et al.*, 1999) where HDMR expansions up to second-order are often sufficient to describe the outputs of many realistic systems.

In this work, cut-HDMR procedure is used to develop a new computational method for predicting the failure probability of structural or mechanical systems subjected to random loads and material properties. With cut-HDMR method, first a reference point $c = \{c_1, c_2, \ldots, c_N\}$ is defined in the variable space. In the convergence limit, cut-HDMR is invariant to the choice of reference point c. In practice, c is chosen within the neighborhood of interest in the input space. The expansion functions are determined by evaluating the input-output responses of the system relative to the defined reference point c along associated lines, surfaces, subvolumes, etc. (*i.e.* cuts) in the input variable space. This process reduces to the following relationship for the component functions in equation (1):

$$g_0 = g(c), \tag{2}$$

$$g_i(x_i) = g(x_i, c^i) - g_0, \tag{3}$$

$$g_{i_1 i_2}(x_{i_1}, x_{i_2}) = g(x_{i_1}, x_{i_2}, c^{i_1 i_2}) - g_{i_1}(x_{i_1}) - g_{i_2}(x_{i_2}) - g_0, \tag{4}$$

where the notation $g(x_i, c^i) = g(c_1, c_2, \ldots, c_{i-1}, x_i, c_{i+1}, \ldots, c_N)$ denotes that all the input variables are at their reference point values except x_i. The g_0 term is the output response of the system evaluated at the reference point c. The higher order terms are evaluated as cuts in the input variable space through the reference point. Therefore, each first-order term $g_i(x_i)$ is evaluated along its variable axis through the reference point. Each second-order term $g_{i_1 i_2}(x_{i_1}, x_{i_2})$ is evaluated in a plane defined by the binary set of input variables x_{i_1}, x_{i_2} through the reference point, etc. The process of subtracting off the lower order expansion functions removes their dependence to assure a unique contribution from the new expansion function.

Formulation of factorized HDMR

In the previous section, the response function $g(x)$ is represented as few low order component functions of HDMR in an additive form. However, when the response function $g(x)$ is dominantly of multiplicative nature, HDMR approximation may not be sufficient to accurately estimate the probabilistic characteristics of the system. The basic purpose of this work is to obtain the general structure of a multiplicative type response function $g(x)$. Multiplicative form of HDMR for a given multivariate limit state/performance function $g(x)$ can be represented as (Tunga and Demiralp, 2004, 2005):

$$g(x) = r_0 \left[\prod_{i=1}^{N} (1 + r_i(x_i)) \right] \left[\prod_{\substack{i_1, i_2 = 1 \\ i_1 < i_2}}^{N} (1 + r_{i_1 i_2}(x_{i_1}, x_{i_2})) \right] \tag{5}$$

$$\times \cdots \times [1 + r_{12 \ldots N}(x_1, x_2, \ldots, x_N)],$$

where r_0 is a constant term, $r_i(x_i)$ is a first-order term expressing the effect of variable x_i acting alone, although generally nonlinearly, upon the output $g(x)$. The function $r_{i_1 i_2}(x_{i_1}, x_{i_2})$ is a second-order term which describes the cooperative effects of the variables x_{i_1} and x_{i_2} upon the output $g(x)$ and so on. The constant term, the first-order term, and the higher order terms can be found by comparing equation (5) with equation (1) (Tunga and Demiralp, 2004). This process reduces to the following relationship for the component functions in equation (5):

$$r_0 = g_0, \tag{6}$$

$$r_i(x_i) = \frac{g_i(x_i)}{g_0}, \tag{7}$$

$$r_{i_1 i_2}(x_{i_1}, x_{i_2}) = \frac{g_0 g_{i_1 i_2}(x_{i_1}, x_{i_2}) - g_{i_1}(x_{i_1}) g_{i_2}(x_{i_2})}{(g_0 + g_{i_1}(x_{i_1}))(g_0 + g_{i_2}(x_{i_2}))}, \tag{8}$$

where, g_0, $g_i(x_i)$ and $g_{i_1 i_2}(x_{i_1}, x_{i_2})$ are defined in equations (2)-(4) of Section 2. The component functions defined in equations (6)-(8) can be further simplified as follows:

$$r_0 = g(c), \tag{9}$$

$$r_i(x_i) = \frac{g(x_i, c^i)}{g(c)} - 1, \tag{10}$$

$$r_{i_1 i_2}(x_{i_1}, x_{i_2}) = \frac{g(c) g(x_{i_1}, x_{i_2}, c^{i_1 i_2})}{g(x_{i_1}, c^{i_1}) g(x_{i_2}, c^{i_2})} - 1. \tag{11}$$

Once all the relevant component functions in equation (5) are determined and suitably represented, then the component functions constitute factorized form of HDMR called FHDMR (Tunga and Demiralp, 2005). Therefore, first- and second-order approximation $\tilde{g}(x)$ of the original implicit response function $g(x)$ can be represented as:

$$\tilde{g}(x) = g(c) \left[\prod_{i=1}^{N} \frac{g(x_i, c^i)}{g(c)} \right], \tag{12}$$

$$\tilde{g}(x) = g(c) \left[\prod_{i=1}^{N} \frac{g(x_i, c^i)}{g(c)} \right] \left[\prod_{\substack{i_1, i_2 = 1 \\ i_1 < i_2}}^{N} \frac{g(c) g(x_{i_1}, x_{i_2}, c^{i_1 i_2})}{g(x_{i_1}, c^{i_1}) g(x_{i_2} c^{i_2})} \right]. \tag{13}$$

Response surface generation
Response surface generation using HDMR in equation (1) is exploited in a previous study (Chowdhury *et al.*, 2008). In this paper, the formulation of response surface using

FHDMR is discussed. Similar to the HDMR, FHDMR in equation (5) is also exact along any of the cuts, and the output response $g(x)$ at a point $\boldsymbol{x}$ off of the cuts can be obtained by following the procedure in step 1 and step 2 below:

Step 1
Interpolate each of the low dimensional HDMR expansion terms with respect to the input values of the point x. For example, consider the first-order component function $g(x_i, c^i) = g(c_1, c_2, \ldots, c_{i-1}, x_i, c_{i+1}, \ldots, c_N)$. If for $x_i = x_i^j$, n function values:

$$g\left(x_i^j, c^i\right) = g\left(c_1, \ldots, c_{i-1}, x_i^j, c_{i+1}, \ldots, c_N\right), \quad j = 1, 2, \ldots, n, \tag{14}$$

are given along the variable x_i-axis, the function value for arbitrary x_i can be obtained by the MLS interpolation (Lancaster and Salkauskas, 1986) as:

$$g\left(x_i, c^i\right) = \sum_{j=1}^n \phi_j(x_i) g'\left(x_i^j, c^i\right), \tag{15}$$

where:

$$\left\{ \begin{array}{c} g'\left(x_i^1, c^i\right) \\ \vdots \\ \vdots \\ g'\left(x_i^n, c^i\right) \end{array} \right\} = \left[\begin{array}{cccc} \phi_1\left(x_i^1\right) & \phi_2\left(x_i^1\right) & \ldots & \phi_n\left(x_i^1\right) \\ \vdots & \vdots & \vdots & \vdots \\ \vdots & \vdots & \vdots & \vdots \\ \phi_1\left(x_i^n\right) & \phi_2\left(x_i^n\right) & \ldots & \phi_n\left(x_i^n\right) \end{array} \right]^{-1} \left\{ \begin{array}{c} g\left(x_i^1, c^i\right) \\ \vdots \\ \vdots \\ g\left(x_i^n, c^i\right) \end{array} \right\}. \tag{16}$$

Similarly, consider the second-order component function $g\left(x_{i_1}, x_{i_2}, c^{i_1 i_2}\right)$ $= g(c_1, \ldots, c_{i_1-1}, x_{i_1}, c_{i_1+1}, \ldots, c_{i_2-1}, x_{i_2}, c_{i_2+1}, \ldots, c_N)$. If for $x_{i_1} = x_{i_1}^{j_1}$ and $x_{i_2} = x_{i_2}^{j_2}$, n^2 function values:

$$g\left(x_{i_1}^{j_1}, x_{i_2}^{j_2}, c^{i_1 i_2}\right) = g\left(c_1, \ldots, c_{i_1-1}, x_{i_1}^{j_1}, c_{i_1+1}, \ldots, c_{i_2-1}, x_{i_2}^{j_2}, c_{i_2+1}, \ldots, c_N\right);$$
$$j_1 = 1, 2, \ldots, n, \ \ j_2 = 1, 2, \ldots, n \tag{17}$$

are given on a grid formed by taking n number of sample points along each of the variable x_{i_1}, and x_{i_2} axis, the function value for arbitrary (x_{i_1}, x_{i_2}) can be obtained by the MLS interpolation (Lancaster and Salkauskas, 1986) as:

$$g\left(x_{i_1}, x_{i_2}, c^{i_1 i_2}\right) = \sum_{j_1=1}^n \sum_{j_2=1}^n \phi_{j_1 j_2}\left(x_{i_1}, x_{i_2}\right) g'$$
$$\times \left(c_1, \ldots, c_{i_1-1}, x_{i_1}^{j_1}, c_{i_1+1}, \ldots, c_{i_2-1}, x_{i_2}^{j_2}, c_{i_2+1}, \ldots, c_N\right), \tag{18}$$

where:

$$
\left\{
\begin{array}{c}
g'\left(x_{i_1}^1, x_{i_2}^1, c^{i_1 i_2}\right) \\
\vdots \\
g'\left(x_{i_1}^1, x_{i_2}^n, c^{i_1 i_2}\right) \\
\vdots \\
g'\left(x_{i_1}^n, x_{i_2}^n, c^{i_1 i_2}\right)
\end{array}
\right\}
=
\left[
\begin{array}{ccccc}
\phi_{11}\left(x_{i_1}^1, x_{i_2}^1\right) & \cdots & \phi_{1n}\left(x_{i_1}^1, x_{i_2}^1\right) & \cdots & \phi_{nn}\left(x_{i_1}^1, x_{i_2}^1\right) \\
\vdots & \vdots & \vdots & \vdots & \vdots \\
\phi_{11}\left(x_{i_1}^1, x_{i_2}^n\right) & \cdots & \phi_{1n}\left(x_{i_1}^1, x_{i_2}^n\right) & \cdots & \phi_{nn}\left(x_{i_1}^1, x_{i_2}^n\right) \\
\vdots & \vdots & \vdots & \vdots & \vdots \\
\phi_{11}\left(x_{i_1}^n, x_{i_2}^n\right) & \cdots & \phi_{1n}\left(x_{i_1}^n, x_{i_2}^n\right) & \cdots & \phi_{nn}\left(x_{i_1}^n, x_{i_2}^n\right)
\end{array}
\right]^{-1}
$$

$$
\times
\left\{
\begin{array}{c}
g\left(x_{i_1}^1, x_{i_2}^1, c^{i_1 i_2}\right) \\
\vdots \\
g\left(x_{i_1}^1, x_{i_2}^n, c^{i_1 i_2}\right) \\
\vdots \\
g\left(x_{i_1}^n, x_{i_2}^n, c^{i_1 i_2}\right)
\end{array}
\right\}.
\tag{19}
$$

In the above equations the interpolation functions $\phi_j(x_i)$ and $\phi_{j_1 j_2}(x_{i_1}, x_{i_2})$ can be obtained using the MLS interpolation scheme (Lancaster and Salkauskas, 1986).

By using equation (15), $g_i(x_i)$ can be generated if n function values are given at corresponding sample points. Similarly, by using equation (18), $g_{i_1 i_2}(x_{i_1}, x_{i_2})$ can be generated if n^2 function values at corresponding sample points are given. The same procedure shall be repeated for all the first-order component functions, i.e. $g_i(x_i)$; $i = 1, 2, \ldots, N$ and the second-order component functions, i.e. $g_{i_1 i_2}(x_{i_1}, x_{i_2})$; $i_1, i_2 = 1, 2, \ldots, N$.

Step 2
Multiply the interpolated values of HDMR expansion terms from zeroth-order to the highest order retained in keeping with the desired accuracy. This leads to first-order FHDMR approximation of the function $g(x)$ as:

$$
\tilde{g}(x) = g(c) \left[\prod_{i=1}^{N} \frac{\sum_{j=1}^{n} \phi_j(x_i) g'\left(c_1, \ldots, c_{i-1}, x_i^j, c_{i+1}, \ldots, c_N\right)}{g(c)} \right],
\tag{20}
$$

and second-order approximation of the function $g(x)$ as:

$$\tilde{g}(x) = g(c) \left[\prod_{i=1}^{N} \frac{\sum_{j=1}^{n} \phi_j(x_i) g'\left(x_i^j, c^i\right)}{g(c)} \right]$$

$$\times \left[\prod_{\substack{i_1,i_2=1 \\ i_1<i_2}}^{N} \frac{g(c)\sum_{j_1=1}^{n}\sum_{j_2=1}^{n} \phi_{j_1 j_2}\left(x_{i_1}, x_{i_2}\right) g'\left(x_{i_1}^{j_1}, x_{i_2}^{j_2}, c^{i_1 i_2}\right)}{\left(\sum_{j_1=1}^{n} \phi_{j_1}\left(x_{i_1}\right) g'\left(x_{i_1}, c^{i_1}\right)\right)\left(\sum_{j_2=1}^{n} \phi_{j_2}\left(x_{i_2}\right) g'\left(x_{i_2}, c^{i_2}\right)\right)} \right]. \tag{21}$$

If n is the number of sample points taken along each of the variable axis and s is the order of the component function considered, starting from zeroth-order to lth order, then total number of function evaluation for interpolation purpose is given by, $\sum_{s=0}^{l}(N!(n-1)^s)/((N-s)!s!)$ which grows polynomially with n and s. As a few low order component functions of HDMR or FHDMR are used, the sample savings due to HDMR or FHDMR are significant compared to traditional sampling. Hence uncertainty analysis using HDMR relies on an accurate reduced model being generated with a small number of full model simulations. An arbitrarily large sample Monte Carlo analysis can be performed on the outputs approximated by HDMR or FHDMR which result in the same distributions as obtained through the Monte Carlo analysis of the full model. The tremendous computational savings result from just having to perform interpolation instead of full model simulations for output determination.

Moving least squares approximation

Consider a function, $u(x)$ over a domain, $\Omega \subseteq \Re^K$, where $K = 1, 2$, or 3. Let $\Omega_x \subseteq \Omega$ denote a sub-domain describing the neighborhood of a point, $x \in \Re^K$ located in Ω. According to the MLS (Lancaster and Salkauskas, 1986), the approximation, $u^h(x)$ of $u(x)$ is:

$$u^h(x) = \sum_{i=1}^{m} p_i(x) a_i(x) = \mathbf{p}^T(x)\mathbf{a}(x), \tag{22}$$

where $\mathbf{p}^T = \{p_1(x), p_2(x), \ldots, p_m(x)\}$ is a vector of complete basis functions of order m and $\mathbf{a}(x) = \{a_1(x), a_2(x), \ldots, a_m(x)\}$ is a vector of unknown parameters that depend on x. The basis functions should satisfy the following properties:

(1) $p_1(x) = 1$;
(2) $p_i(x) \in C^s(\Omega), \quad i = 1, 2, \ldots, m$ where $C^s(\Omega)$ is a set of functions that have continuous derivatives up to order s on Ω; and
(3) $p_i(x), i = 1, 2, \ldots, m$ constitute a linearly independent set.

For example, in one dimension ($K = 1$) with x_1-coordinate:

$$\boldsymbol{p}^T(x) = \{1, x_1\}, m = 2, \tag{23}$$

representing linear basis function. Similarly, in two dimensions ($K = 2$) with x_1- and x_2-coordinates linear basis function is:

$$\boldsymbol{p}^{\mathrm{T}}(x) = \{1, x_1, x_2\}, \quad m = 3, \tag{24}$$

In equation (22), the coefficient vector, $\mathbf{a}(x)$ is determined by minimizing a weighted discrete L_2 norm, defined as:

$$J(x) = \sum_{I=1}^{n_I} w_I(x)[\mathbf{p}^{\mathrm{T}}(x_I)\mathbf{a}(x) - d_I]^2 = [\mathbf{Pa}(x) - \mathbf{d}]^{\mathrm{T}}\mathbf{W}[\mathbf{Pa}(x) - \mathbf{d}], \tag{25}$$

where x_I denotes the coordinates of sample point I, $\boldsymbol{d}^{\mathrm{T}} = \{d_1, d_2, \ldots, d_{n_I}\}$ with d_I representing the nodal parameter (not the nodal values of $u^h(x)$) for sample point I, $\mathbf{W} = \mathrm{diag}[w_1(x), w_2(x), \ldots, w_{n_t}(x)]$ with $w_I(x)$ denoting the weight function associated with sample point I such that $w_I(x) \geq 0$ for all x in the support Ω_x of $w_I(x)$ and zero otherwise, n_t is the number of sample points in the domain Ω, and:

$$\boldsymbol{P} = \begin{bmatrix} \boldsymbol{p}^{\mathrm{T}}(x_1) \\ \boldsymbol{p}^{\mathrm{T}}(x_2) \\ \vdots \\ \boldsymbol{p}^{\mathrm{T}}(x_{n_t}) \end{bmatrix} \in \mathrm{L}\big(\mathfrak{R}^{n_t} \times \mathfrak{R}^m\big). \tag{26}$$

A number of weight functions are available in the literature (Singh, 2004; Rao and Rahman, 2000). In this study, a weight function proposed by Rao and Rahman (2000) is used, which is defined as:

$$w_I(x) = \begin{cases} \dfrac{\left(1+\gamma^2\dfrac{z_I^2}{z_{mI}^2}\right)^{-\left(\frac{1+\gamma}{2}\right)} - (1+\gamma^2)^{-\left(\frac{1+\gamma}{2}\right)}}{1-(1+\gamma^2)^{-\left(\frac{1+\gamma}{2}\right)}}, & z_I \leq z_{mI}, \\ \\ 0, & z_I > z_{mI}, \end{cases} \tag{27}$$

where γ is a parameter controlling the shape of the weight function, $z_I = |x - x_I|$ distance from a point x to sample point I, and Z_{mI} is the domain of influence of sample point I. In the numerical examples presented in this paper the domain of influence Z_{mI} is chosen to be 2.01 for all sample points. The stationarity of $\mathbf{J}(x)$ with respect to $a(x)$ yields:

$$\mathbf{A}(x)\mathbf{a}(x) = \mathbf{C}(x)\mathbf{d}, \tag{28}$$

where:

$$\mathbf{A}(x) = \sum_{I=1}^{n_t} w_I(x)p(x_I)\mathbf{p}^{\mathrm{T}}(x_I) = \mathbf{P}^{\mathrm{T}}\mathbf{W}\mathbf{P}, \tag{29}$$

$$\mathbf{C}(x) = [w_1(x)p(x_1), \ldots, w_n(x)p(x_n)] = \mathbf{P}^T\mathbf{W}. \tag{30}$$

Solving $a(x)$ from equation (28) and then substituting it in equation (22) gives:

$$u^h(x) = \sum_{I=1}^{n_t} \phi_I(x)d_I = \Phi^{\mathrm{T}}(x)d, \tag{31}$$

where:

$$\Phi^{\mathrm{T}}(x) = \{\phi_1(x), \phi_2(x), \ldots, \phi_{n_t}(x)\} = \mathbf{p}^{\mathrm{T}}(x)\mathbf{A}^{-1}(x)\mathbf{C}(x), \tag{32}$$

is a vector with its Ith component:

$$\phi_I(x) = \sum_{j=1}^{m} p_j(x)[A^{-1}(x)C(x)]_{jI}, \tag{33}$$

representing the interpolation function of the MLS approximation corresponding to sample point I.

Failure probability estimation
Equations (20) and (21) provide, respectively, first- and second-order FHDMR approximation $\tilde{g}(x)$ of the original implicit limit state/performance function $g(x)$ using the MLS interpolation functions, constant $g(c)$ term, first-order $g\left(c_1, \ldots, c_{i-1}, x_i^j, c_{i+1}, \ldots, c_N\right)$ and second-order $g(c_1, \ldots, c_{i_1-1}, x_{i_1}^{j_1}, c_{i_1+1}, \ldots, c_{i_2-1}, x_{i_2}^{j_2}, c_{i_2+1}, \ldots, c_N)$ HDMR terms. Therefore, the failure probability P_{F} can be easily estimated by performing MCS on first- or second-order approximation $\tilde{g}(x)$ of the original implicit limit state/performance function $g(x)$ and is given by:

$$P_{\mathrm{F}} = \frac{1}{N_{\mathrm{S}}} \sum_{i=1}^{N_{\mathrm{S}}} I\left[\tilde{g}(x^i) < 0\right], \tag{34}$$

where x^i is ith realization of $\mathbf{X}$, N_{S} is the sampling size, $I[.]$ is a deciding function of fail or safe state such that $I = 1$, if $\tilde{g}(x^i) < 0$ otherwise zero. Flow diagram of the computational process using HDMR and FHDMR and the failure probability P_{F} estimation by MCS are shown in Figures 1 and 2, respectively. Since first- and second-order FHDMR approximation leads to explicit representation of the original implicit limit state/performance function, MCS can be conducted for any sampling size. The total cost of original function evaluation entails a maximum of $(n-1) \times N + 1$ and $(n-1)^2(N-1)N/2 + (n-1)N + 1$ by the present method using first- and second-order HDMR/FHDMR approximation, respectively.

**Numerical examples**
Five numerical examples involving structural/solid-mechanics and geo-technical engineering problems are presented to illustrate the performance of HDMR and FHDMR approximation. An exact continuous function to replace a univariate or multivariate piece wise continuous function may not always be available in general problems. Rather that seeking an exact continuous function to replace a piece wise continuous function, an equivalent continuous function can be found based on present methods.

The estimated failure probabilities are compared through the following five procedures:
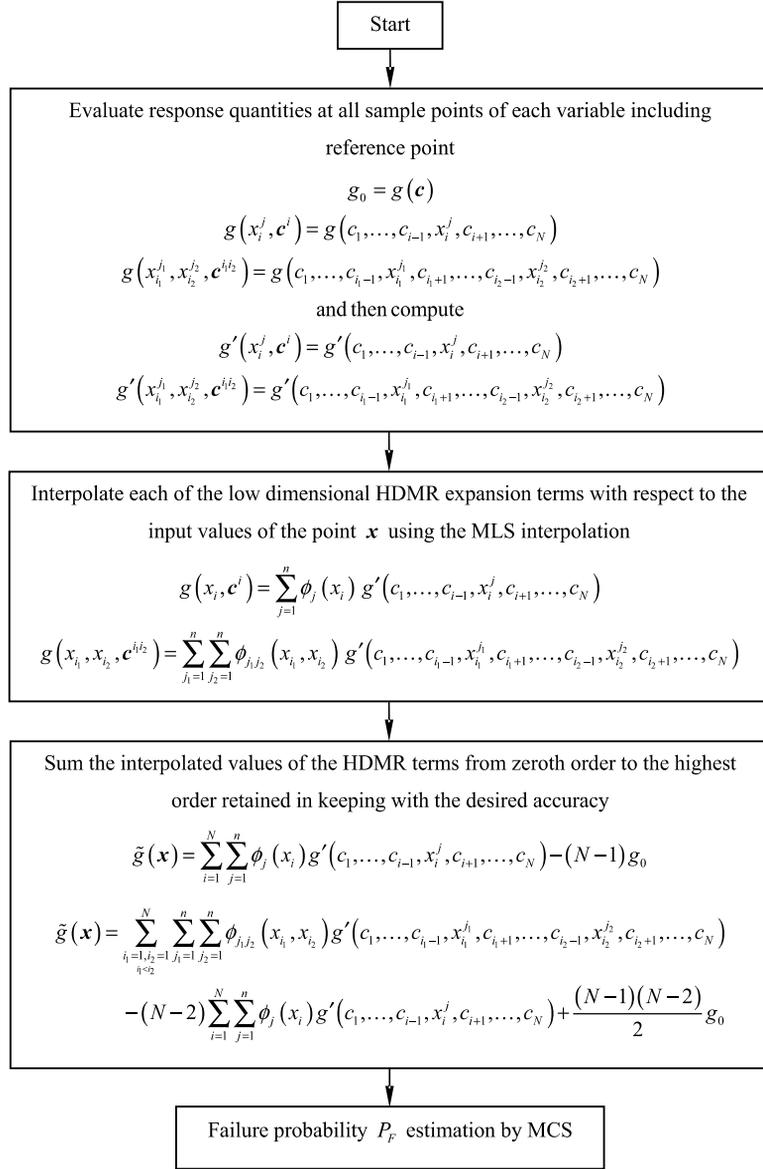
Figure 1.
Flowchart of failure
probability P_F estimation
using HDMR
approximation

(1) *Method 1*. Direct MCS using the exact limit state/performance function, which may be implicitly defined. This is assumed to be the true failure probability and is used to benchmark other methods.

(2) *Method 2*. Failure probability estimation using first-order FHDMR approximation.
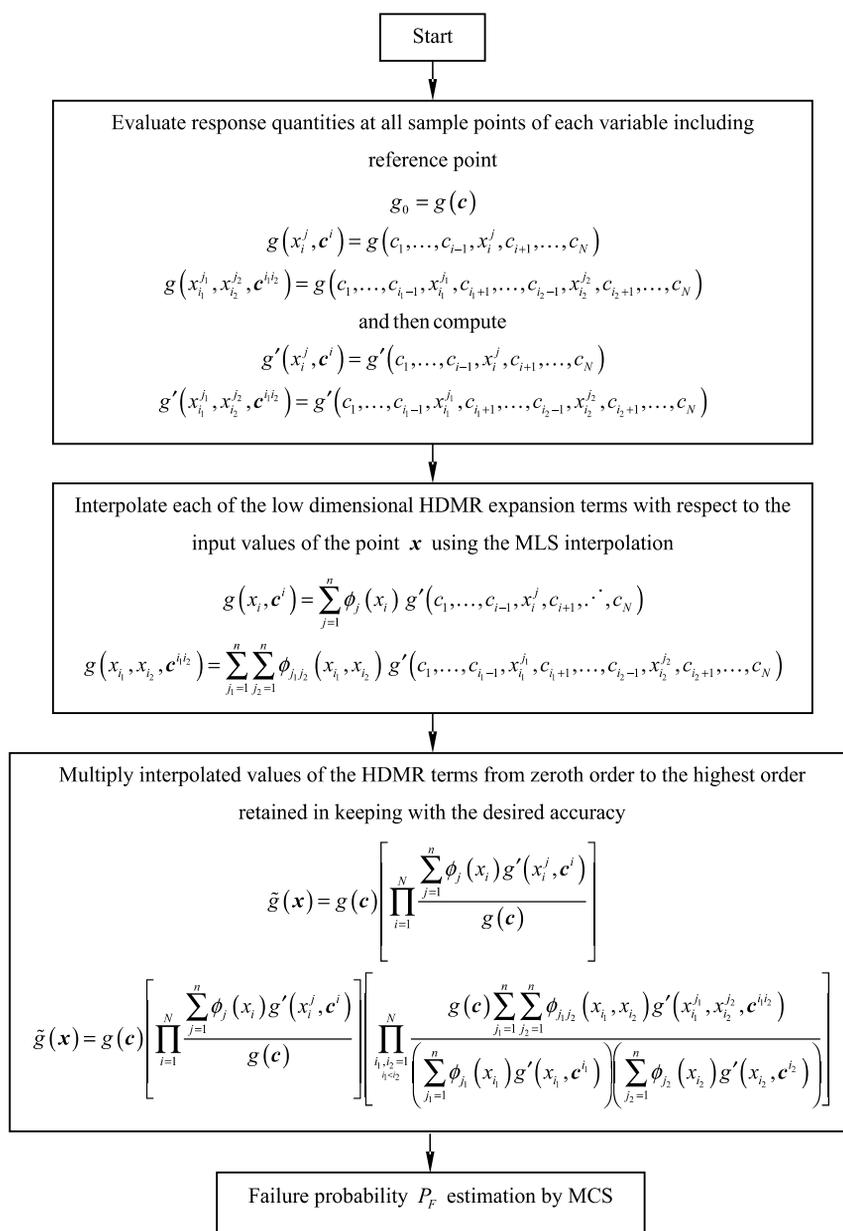
Figure 2.
Flowchart of failure
probability P_F estimation
using FHDMR
approximation

(3) *Method 3*. Failure probability estimation using first-order HDMR approximation.

(4) *Method 4*. Failure probability estimation using second-order FHDMR approximation.

(5) Failure probability estimation using second-order HDMR approximation.

The coefficient of variation δ of the estimated failure probability P_F by direct MCS for the sampling size N_S considered is computed using:

$$\delta = \sqrt{\frac{(1 - P_F)}{N_S P_F}}. \tag{35}$$

When comparing computational efforts by various methods in evaluating the failure probability P_F, the number of original limit state/performance function evaluations is chosen as the primary comparison tool in this paper. This is because of the fact that, number of function evaluations indirectly indicates the CPU time usage. For direct MCS, number of original function evaluations is same as the sampling size. While evaluating the failure probability P_F through direct MCS, CPU time is more because it involves number of repeated actual finite-element analysis. However, in the present methods MCS is conducted in conjunction with Methods 2-5. Here, although the same sampling size as in direct MCS is considered, the number of original function evaluation is very less. Hence, the computational effort expressed in terms of function evaluations alone should be carefully interpreted for problems involving explicit functions. For Methods 2 and 3, equally spaced sample points are deployed along the variable axis through the reference point. Sampling schemes for first- and second-order HDMR/FHDMR approximation are explained in Figures 3 and 4.

Example 1. Cantilever beam
A cantilever beam subjected to a tip load P is considered in this example. The limit state/performance function is defined as tip displacement should be less than 0.15 in:
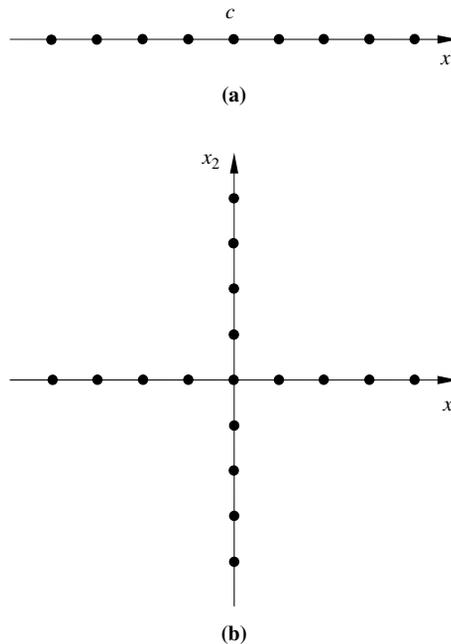
Figure 3.
Sampling scheme for first-order HDMR/FHDMR. For a function having (a) one variable (x); (b) two variables (x_1 and x_2)
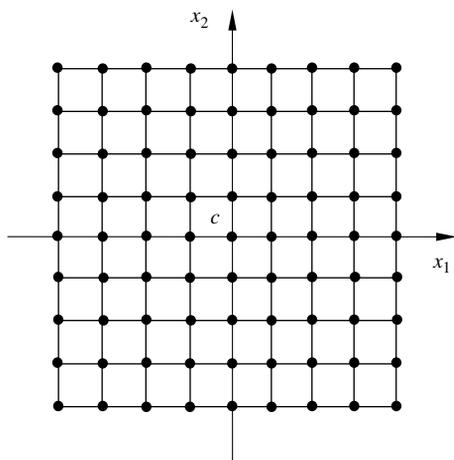
Figure 4.
Sampling scheme for
second-order
HDMR/FHDMR for a
function having two
variables (x_1 and x_2)

$$g(x) = 0.15 - \frac{4Pl^3}{Ebh^3}, \tag{36}$$

where P is tip load and b, h, l are width, height and length of the beam, which are considered as random variables. The mean values of the random variables are 30 in, 0.8359 in and 2.5093 in, respectively, and standard deviations are 3 in, 0.08 in and 0.25 in, respectively, for width, height and length of the beam. Young's modulus, E of the beam is 10^7 psi. Both length and height are considered as log-normally distributed and width is considered as a Gaussian. For evaluating the failure probability P_F, seven equally spaced sample points ($n = 7$) are deployed along each of the variable axis to form first-order approximation using Methods 2 and 3. The reference point is taken as the mean values of the random variables. Figure 5 compares the variation of the failure probability with tip load obtained by different methods. A sample size of 10^5 is considered in direct MCS to evaluate the failure probability P_F, which ranges from
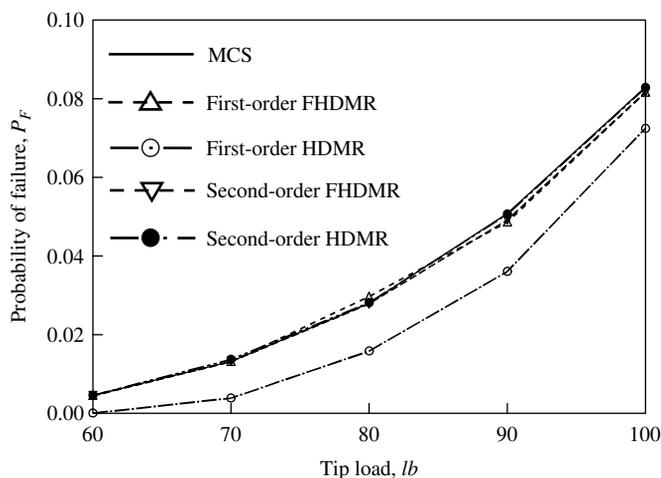
Figure 5.
Variation of failure
probability with tip load
(Example 1)

0.00502 to 0.08310 and the COV of P_F corresponding to this sample size varies from 0.045 to 0.011 (computed using equation (35)) when tip load P varies from 60 to 100 lb. The estimated failure probability reported in Figure 5 using Methods 1-3 are 0.0284, 0.0301 and 0.0163, respectively, when tip load $P = 80$ lb. It can be observed that, Method 2 overestimates the failure probability by 6.14 percent, when compared with direct MCS results, while Method 3 underpredicts by 42.45 percent. Accumulation of large amount of error using Method 3, may perhaps be due to neglecting the higher order cooperative effects and multiplicative nature of the limit state/performance function. However, both Methods 2 and 3 needs only 19 function evaluations, while direct MCS requires 10^5 number of original function evaluations, respectively.

Seven equally spaced sample points ($n = 7$) along each of the variable axis is selected to form a regular grid, for construction of second-order approximation using Methods 4 and 5. The reference point is taken as the mean values of the random variables. Figure 5 also presents the variation of the failure probability P_F with tip load and the associated computational effort in terms of number of function evaluations obtained using Methods 4 and 5. It can be observed from Figure 5 that Method 4 almost exactly estimates the failure probability ($P_F = 0.02831$) compared with the benchmark result of direct MCS ($P_F = 0.02836$) when tip load $P = 80$ lb. The results obtained using Method 5 ($P_F = 0.02853$) closely matches with direct MCS estimate ($P_F = 0.02836$) and also closer to Method 2 ($P_F = 0.0301$). This is attributed to consideration of the second-order cooperative effects in function approximation. For tip load $P = 80$ lb, compared to the result obtained using Method 1 ($P_F = 0.02836$), Method 5 produces much closer estimate of the failure probability ($P_F = 0.02853$) than the result obtained using Method 3 ($P_F = 0.0163$). But the number of function evaluations required using Methods 4 and 5 are 127 compared with 19 function evaluations for Methods 2 and 3. Therefore, to make a balance between the computational cost in terms of function evaluations and the accuracy, Method 2 seems most suitable, especially for multiplicative nature of the limit state/performance function.

The effect of number of sample points used for function approximation on the reliability estimation is examined by carrying a similar analysis varying n form 3 to 9. Figure 6 (a) and (b) presents, respectively, the variation of the reliability index β and the estimated failure probability P_F with respect to number of sample points, for tip load $P = 80$ lb. In Method 2, P_F ranges from 0.0118 (-58.39 percent) (at $n = 3$) to 0.0325 ($+14.59$ percent) (at $n = 9$), whereas P_F ranges from 0.0011 (-96.12 percent) (at $n = 3$) to 0.0165 (-41.89 percent) (at $n = 9$) using Method 3. Similarly, using Method 4, P_F ranges from 0.0280 (-1.23 percent) (at $n = 3$) to 0.0283 ((0.07 percent) (at $n = 9$), whereas P_F ranges from 0.0286 ($+1.02$ percent) (at $n = 3$) to 0.0284 ($+0.14$ percent) (at $n = 9$) using Method 5. Compared with direct MCS, error in the estimated failure probability using different methods is tabulated in Table I. Table I shows that, Method 2 resulted in drastic reduction of approximation error of the estimated failure probability from -96.12 to -58.39 percent for $n = 3$, from -55.75 to $+6.49$ percent for $n = 5$, from -42.45 to $+6.14$ percent for $n = 7$, and from -41.89 to $+14.59$ percent for $n = 9$ compared with Method 3. Similarly, compared with Method 3, Method 5 also resulted in drastic reduction of approximation error of the estimated failure probability from -96.12 to $+1.02$ percent for $n = 3$, from -55.75 to $+0.67$ percent for $n = 5$, from -42.45 to $+0.59$ percent for $n = 7$, and from -41.89 to $+0.14$ percent for $n = 9$. Similar trend is found by comparing the results obtained using Methods 2 and 4 and also comparing the results obtained using
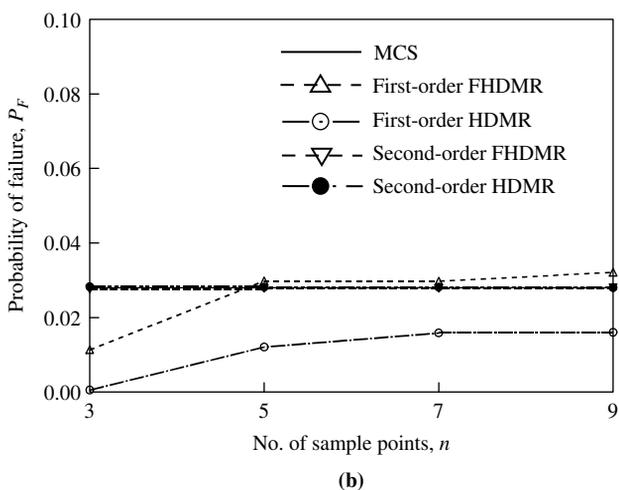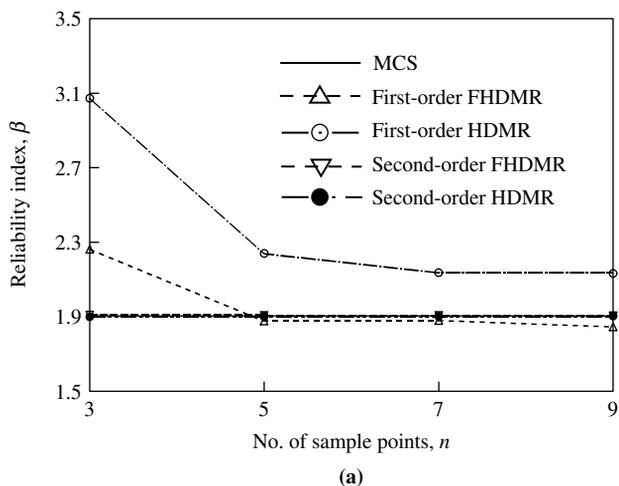
Figure 6.
Variation of reliability
estimation (Example 1).
(a) Reliability index, β;
(b) probability of failure,
P_F

Method	Number of sample points (n)			
	3	5	7	9
First-order FHDMR (percent)	− 58.39	+ 6.49	+ 6.14	+ 14.59
First-order HDMR (percent)	− 96.26	− 55.75	− 42.45	− 41.89
Second-order FHDMR (percent)	− 1.23	− 0.25	− 0.18	− 0.07
Second-order HDMR (percent)	+ 1.02	+ 0.67	+ 0.59	+ 0.14

Table I.
Estimation of error using
different methods for
Example 1

724

Methods 3 and 4. However, the computational effort in terms of number of function evaluations for second-order HDMR and FHDMR approximation (Methods 4 and 5) increased from 7 to 19 for $n = 3$, from 13 to 61 for $n = 5$, from 19 to 127 for $n = 7$, and from 25 to 217 for $n = 9$, when compared with first-order (Methods 2 and 3).

Example 2. Ten bar truss structure

A 10-bar, linear-elastic, truss structure, shown in Figure 7, considered in this example to examine the accuracy and efficiency of the proposed reliability method. The Young's modulus of the material is 10^7 psi. Two concentrated forces of 10^5 lb are applied at nodes 2 and 3, as shown in Figure 7. The cross-sectional area $x_i, i = 1, 2, \ldots, 10$ for each bar follows normal distribution and has mean $\mu = 2.5$ in^2 and standard deviation $\sigma = 0.5$ in^2. The limit state/performance function considered here is the eigenvalue limit. The eigenvalue must be greater than 9.30 (rad/s^2). Hence, the limit state/performance function is defined as:

$$g(x) = 1.0 - \frac{\text{Fundamental eigenvalue}}{9.30} \geq 0.0 \text{(Failure)}. \tag{37}$$

For evaluating the failure probability P_F, seven equally spaced sample points ($n = 7$) are deployed along each of the variable axis to form approximation using Methods 2 and 3. The reference point c is taken as mean values of the random variables. Table II
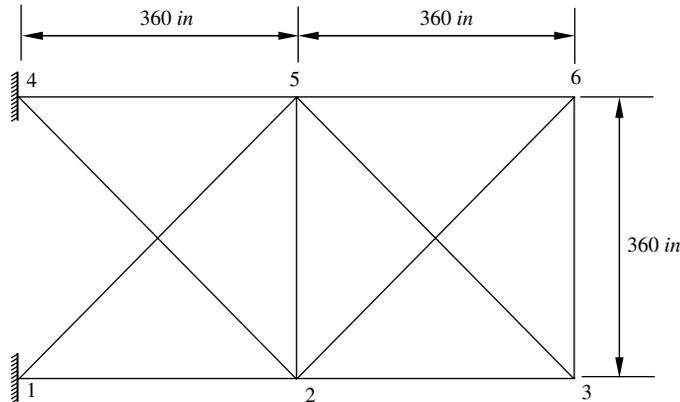
Figure 7.
Ten bar truss structure for Example 2

Method	Failure probability	Number of function evaluation[*]
Direct Monte Carlo simulation	0.10627	100,000
First-order FHDMR	0.09968	61[**]
First-order HDMR	0.09737	61[**]
Second-order FHDMR	0.10625	1681[***]
Second-order HDMR	0.10453	1681[***]

Table II.
Estimation of failure probability for Example 2

Notes: [*]Total number of times the original performance function is calculated.; [**]$(n-1) \times N + 1 = (7-1) \times 10 + 1 = 61$; [***]$(n-1)^2(N-1)N/2 + (n-1)N + 1 = (7-1)^2 + (7-1)10 + 1 = 1681$

compares the results obtained by Method 2, Method 3, and direct MCS. A sampling size $N_S = 10^5$ is considered in direct MCS to estimate the failure probability P_F. The COV of P_F corresponding to this sampling size is 0.0025 (computed using equation (35)). Table II also contains the computational effort in terms of number of function evaluations, associated with each of the methods. Compared with the failure probability obtained using direct MCS ($P_F = 0.10627$), Methods 2 and 3 underestimates the failure probability by 6.20 percent ($P_F = 0.09968$) and 8.37 percent ($P_F = 0.09737$), respectively. However, Methods 2 and 3 need only 61 function evaluations, while direct MCS requires 10^5 number of original function evaluations, respectively. In an effort to reduce the approximation error further, second-order HDMR and FHDMR approximation is adopted in evaluating the failure probability P_F using the present method. In this case, approximation is constructed using a regular grid formed with seven equally spaced sample points ($n = 7$) along each of the variable axis. The reference point c is taken as mean values of the random variables. Table II also shows the failure probability P_F-value obtained using second-order FHDMR (Method 4) ($P_F = 0.10625$) and second-order HDMR ($P_F = 0.10453$) (Method 5) approximation and the associated computational effort. Methods 4 and 5 resulted in significant reduction in error of the estimated failure probability from -6.20 to -0.02 percent and -8.37 to -1.64 percent, respectively, with an increase in the number of function evaluations from 61 to 1681, as compared with Methods 2 and 3.

The effect of number of sample points used for first- and second-order HDMR and FHDMR approximation on the reliability estimation is examined by carrying a similar analysis varying n form 3 to 9. Figure 8 (a) and (b) presents, respectively, the variation of the reliability index P_F and the estimated failure probability P_F with respect to number of sample points. Using Method 2, P_F ranges from 0.14656 ($+37.91$ percent) (at $n = 3$) to 0.09954 (-6.33 percent) (at $n = 9$), whereas P_F ranges from 0.14971 ($+40.88$ percent) (at $n = 3$) to 0.09719 (-8.54 percent) (at $n = 9$) using Method 3. Similarly, using Method 4, P_F ranges from 0.09954 (-6.33 percent) (at $n = 3$) to 0.10625 (-0.02 percent) (at $n = 9$), whereas P_F ranges from 0.09863 (-7.19 percent) (at $n = 3$) to 0.0284 (-0.56 percent) (at $n = 9$) using Method 5. Compared with direct MCS, error in the estimated failure probability using different methods is tabulated in Table III. It can be noticed that, Method 2 resulted in reduction of approximation error of the estimated failure probability from -40.88 to $+37.91$ percent for $n = 3$, from -5.81 to -3.86 percent for $n = 5$, from -8.37 to -6.20 percent for $n = 7$, and from -8.54 to -6.33 percent for $n = 9$ compared with Method 3. Similarly, compared with Method 3, Method 4 resulted in drastic reduction of approximation error of the estimated failure probability from -40.88 to -6.33 percent for $n = 3$, from -5.81 to -1.90 percent for $n = 5$, from -8.37 to -0.02 percent for $n = 7$, and from -8.54 to -0.02 percent for $n = 9$. Compared with Method 3, Method 5 also resulted in drastic reduction of approximation error of the estimated failure probability from $+40.88$ to -7.19 percent for $n = 3$, from -5.81 to -4.74 percent for $n = 5$, from -8.37 to -1.64 percent for $n = 7$, and from -8.54 to -0.56 percent for $n = 9$. This is attributed mainly to consideration of the cooperative effects in Method 5 for approximation. However, the computational effort in terms of number of function evaluations for second-order HDMR and FHDMR approximation (Methods 4 and 5) increased from 21 to 201 for $n = 3$, from 41 to 761 for $n = 5$, from 61 to 1681 for $n = 7$, and from 81 to 2961 for $n = 9$, when compared with first-order HDMR and FHDMR approximation (Methods 2 and 3).
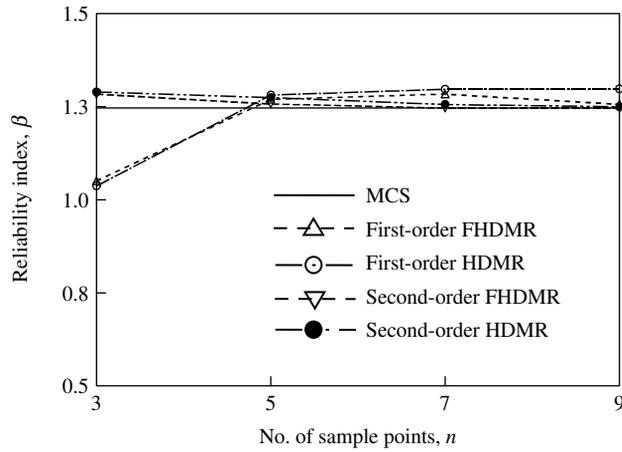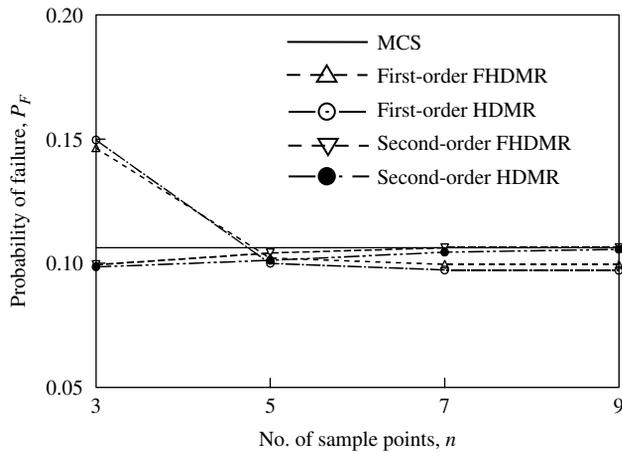
Figure 8.
Variation of reliability
estimation (Example 2).
(a) Reliability index, β;
(b) probability of failure, P_F

Method (percent)	Number of sample points (n)			
	3	5	7	9
First-order FHDMR	+37.91	−3.86	−6.20	−6.33
First-order HDMR	−40.88	−5.81	−8.37	−8.54
Second-order FHDMR	−6.33	−1.90	−0.02	−0.02
Second-order HDMR	−7.19	−4.74	−1.64	−0.56

Table III.
Estimation of error using
different methods for
Example 2

Example 3. Soil settlement problem

This is a practical engineering example studied earlier by Ang and Tang (1975) and Shan and Wang (2006). The settlement of a point A in Figure 9 caused by the construction of a structure can be shown to be primarily caused by the consolidation of the clay layer. Suppose the contribution of settlement due to secondary consolidation is negligible. For normally loaded clay, the settlement S is given by:

$$S = \frac{C_c}{1 + e_0} H \log \frac{p_0 + \Delta p}{p_0},$$ (38)

where C_c C_c is the compression index of the clay; e_0 is the void ratio of the clay layer before loading; H is the thickness of the clay layer; p_0 is the original effective pressure at point B (mid height of the clay layer) before loading; and Δp is the increase in pressure at point B caused by the construction of the structure; "log" denotes logarithm to the base 10. Because of the non-uniform thickness and lack of homogeneity of the clay layer, the settlement predicted by the empirical formula could be subject to uncertainty in predicted settlement.

Suppose satisfactory performance requires that the settlement be less than 2.5 in. The statistical properties of the random variables are presented in Table IV. Determine the probability of excessive settlement at point B in Figure 9. The limit state/performance function is defined as:

$$g(x) = 2.5 - \frac{C_c}{1 + e_0} H \log \frac{p_0 + \Delta p}{p_0}.$$ (39)

For evaluating the failure probability P_F, five equally spaced sample points ($n = 5$) are deployed along each of the variable axis to form approximation using Methods 2 and 3.
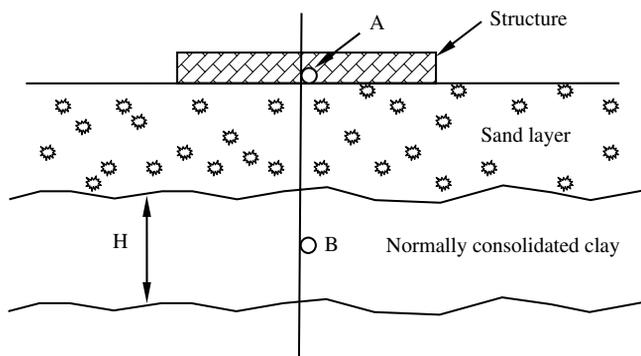
Figure 9.
Soil profile for Example 3

Random variable	Mean	COV	Distribution type
C_c	0.396	0.25	Gaussian
e_0	1.190	0.15	Gaussian
H	168 in	0.05	Gaussian
p_0	3.72 ksf	0.05	Gaussian
Δp	0.50	0.20	Gaussian

Table IV.
Statistical properties of the random variables for Example 3

The reference point c is taken as mean values of the random variables. Table V compares the results obtained by Method 2, Method 3, and direct MCS. A sampling size $N_S = 10_6$ is considered in direct MCS to estimate the failure probability P_F. The COV of P_F corresponding to this sampling size is 0.003 (computed using equation (35)). Table V also contains the computational effort in terms of number of function evaluations, associated with each of the methods. Compared with the failure probability obtained using direct MCS ($P_F = 0.08096$), Methods 2 and 3 underestimates the failure probability by 0.41 percent ($P_F = 0.08063$) and 18.16 percent ($P_F = 0.06625$), respectively. However, Methods 2 and 3 need only 21 function evaluations, respectively, while direct MCS requires 10^6 number of original function evaluations. In addition Table V shows the number of function evaluations and the failure probability estimate reported by Shan and Wang (2006) using failure surface frontier.

In an effort to reduce the approximation error further, second-order HDMR and FHDMR is used in evaluating the failure probability P_F. In this case, approximation of the limit state/performance function is constructed using a regular grid formed with five equally spaced sample points ($n = 5$) along each of the variable axis. The reference point c is taken as mean values of the random variables. Table V also presents the failure probability P_F-value obtained using second-order FHDMR (Method 4) ($P_F = 0.08072$) and second-order HDMR ($P_F = 0.08013$) (Method 5) approximation and the associated computational effort. Methods 4 and 5 resulted in significant reduction in error of the estimated failure probability from -0.41 to -0.29 percent and -18.16 to -1.03 percent, respectively, with an increasing function evaluation from 21 to 181, as compared with Methods 2 and 3.

The effect of number of sample points used for first- and second-order HDMR and FHDMR approximation on the reliability estimation is examined by carrying a similar analysis varying n form 3 to 9. Figure 10 (a) and (b) presents, respectively, the variation of the reliability index β and the estimated failure probability P_F with respect to number of sample points. In Method 2, P_F ranges from 0.06612 (-18.33 percent) (at $n = 3$) to 0.08167 ($+0.88$ percent) (at $n = 9$), whereas P_F ranges from 0.05059 (-37.51 percent) (at $n = 3$) to 0.06742 (-16.72 percent) (at $n = 9$) using Method 3. Similarly, using Method 4, P_F ranges from 0.08001 (-1.17 percent) (at $n = 3$) to 0.08091 (-0.06 percent) (at $n = 9$), whereas P_F ranges from 0.07852 (-3.01 percent) (at $n = 3$) to 0.08081 (-0.18 percent) (at $n = 9$) using Method 5. Compared with direct MCS, error in the estimated failure probability using different methods is tabulated in Table VI. Method 2 resulted in reduction of approximation error of the estimated failure probability from

Method	Failure probability	Number of function evaluation[*]
Direct Monte Carlo simulation	0.08096	100,000
Failure surface frontier (Shan and Wang, 2006)	0.09020	2213
First-order FHDMR	0.08063	21[**]
First-order HDMR	0.06625	21[**]
Second-order FHDMR	0.08072	181[***]
Second-order HDMR	0.08013	181[***]

Table V.
Estimation of failure probability for Example 3

Notes: [*]Total number of times the original performance function is calculated; [**]$(n - 1) \times N + 1 = (5 - 1) \times 5 + 1 = 21$; [***]$(n - 1)^2(N - 1)N /2 + (n - 1) N + 1 = (5 - 1)^2 (5 - 1)5 /2 + (5 - 1)5 + 1 = 181$
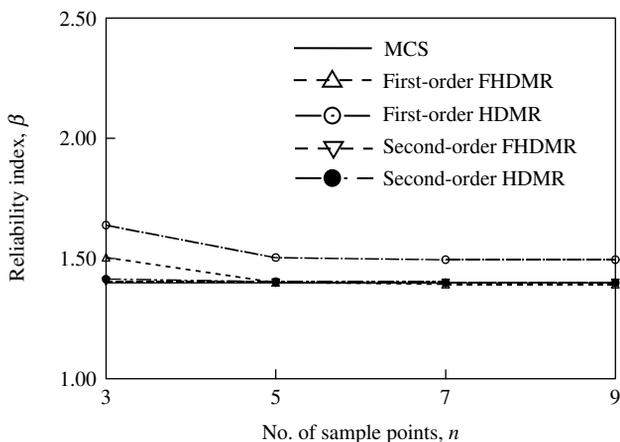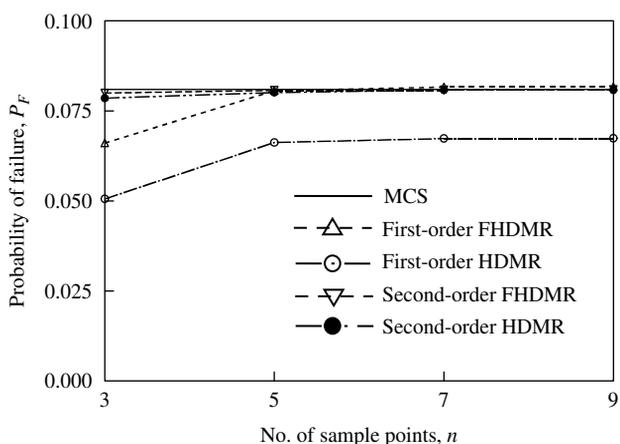
Figure 10.
Variation of reliability
estimation (Example 3).
(a) Reliability index, β; and
(b) probability of failure, P_F

Method (percent)	Number of sample points, n			
	3	5	7	9
First-order FHDMR	-18.33	-0.41	$+0.82$	$+0.88$
First-order HDMR	-37.51	-18.16	-16.78	-16.72
Second-order FHDMR	-1.17	-0.29	-0.08	-0.06
Second-order HDMR	-3.01	-1.03	-0.21	-0.18

Table VI.
Estimation of error using
different methods for
Example 3

-37.51 to -18.33 percent for $n = 3$, from -18.16 to -0.41 percent for $n = 5$, from -16.78 to $+0.82$ percent for $n = 7$, and from -16.72 to $+0.88$ percent for $n = 9$ compared with Method 3. Similar trend is found by comparing the results obtained using Methods 2 and 4, by comparing the results obtained using Methods 3 and 4

and by comparing the results obtained using Methods 3 and 5. However, the computational effort in terms of number of function evaluations for second-order HDMR and FHDMR approximation (Methods 4 and 5) increased from 11 to 51 for $n = 3$, from 21 to 181 for $n = 5$, from 31 to 391 for $n = 7$, and from 41 to 681 for $n = 9$, when compared with first-order HDMR and FHDMR approximation (Methods 2 and 3).

Example 4. Burst margin of rotating disk

Consider an annular disk (Rahman and Wei, 2006) of inner radius R_i, outer radius R_0, shown in Figure 11. The disk is subject to an angular velocity ω about an axis perpendicular to its plane at the center. The ultimate strength material is S_u and material utilization factor is α_m. The burst margin is the safety margin before an overstress condition occurs due to the stress on the part being too large for the material to withstand. The satisfactory performance of the disk is defined when the burst margin M_b, exceeds the threshold value of 0.37473:

$$M_b = \sqrt{\frac{\alpha_m S_u}{\left(\frac{\rho\left(\frac{2\omega\pi}{60}\right)^2 \left(R_o^3 - R_i^3\right)}{3(385.82)(R_o - R_i)}\right)}}. \tag{40}$$

Therefore, the limit state/performance function can be defined as:

$$g(x) = M_b(\alpha_m, S_u, \rho, \omega, R_0, R_i) - 0.37473. \tag{41}$$

The statistical properties of the random variables are listed in Table VII. For evaluating the failure probability P_F, nine equally spaced sample points ($n = 9$) are deployed along each of the variable axis to form first-order HDMR/FHDMR approximation.
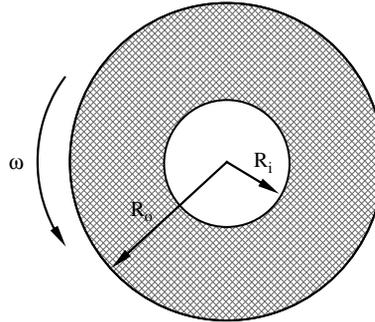

Figure 11.
Rotating disk for
Example 4

Random variable	α_m	S_u (lb/in^2)	ρ (lb/in^2)	ω (rpm)	R_0 (in)	R_i (in)
Distribution	Weibull*	Gaussian	Uniform**	Gaussian	Gaussian	Gaussian
Mean	0.9378	2.20×10^5	0.29	2.10×10^4	24	8
Standard deviation	0.04655	5.0×10^3	0.00577	1.0×10^3	0.50	0.30

Table VII.
Statistical properties of
the random variables of
rotating disk

**Notes:** *Scale parameter = 25.508; shape parameter = 0.958; **Uniformly distributed over (0.28 − 0.3)

The reference point c is taken as mean values of the random variables. Table VIII compares the results obtained by Method 2, Method 3, and direct MCS. A sampling size $N_S = 10^6$ is considered in direct MCS to estimate the failure probability P_F. The COV of P_F corresponding to this sampling size is 0.031 (computed using equation (35)). Table VIII also contains the computational effort in terms of number of function evaluations, associated with each of the methods. Compared with the failure probability obtained using direct MCS ($P_F = 0.00101$), Methods 2 and 3 overestimate the failure probability by 0.99 percent ($P_F = 0.00102$) and 59.41 percent ($P_F = 0.00161$), respectively. However, Methods 2 and 3 need only 49 function evaluations, while direct MCS requires 10^6 number of original function evaluations, respectively. In an effort to reduce the approximation error further, the failure probability P_F is estimated using second-order FHDMR and HDMR approximation. In this case second-order approximation of the function defined in equation (41) is constructed using a regular grid formed with nine equally spaced sample points ($n = 9$) along each of the variable axis. The reference point c is taken as mean values of the random variables. Table VIII also shows the failure probability P_F-value obtained with the present method using second-order FHDMR (Method 4) ($P_F = 0.00101$) and second-order HDMR ($P_F = 0.00102$) (Method 5) approximation and the associated computational effort. Method 4 estimates the exact failure probability, while using Method 5 resulted in significant reduction in error of the estimated failure probability from $+59.41$ percent to $+0.99$ percent with an increasing function evaluation from 49 to 1009, as compared with Method 3. In addition Table V shows the number of function evaluations and the failure probability estimate reported by Rahman and Wei (2006) using MPP(based univariate method.

The effect of number of sample points used for first- and second-order HDMR and FHDMR approximation on the reliability estimation is examined by carrying a similar analysis varying n form 3 to 11. Figure 12 (a) and (b) presents, respectively, the variation of the reliability index β and the estimated failure probability P_F with respect to number of sample points. Using Method 2, P_F ranges from 0.03148 ($+3.016 \times 10^3$ percent) (at $n = 3$) to 0.00096 (-4.95 percent) (at $n = 11$), whereas P_F ranges from 0.03165 ($+3.034 \times 10^3$ percent) (at $n = 3$) to 0.00155 ($+53.46$ percent) (at $n = 11$) using Method 3. Similarly, using Method 4, P_F ranges from 0.00148 ($+46.53$ percent) (at $n = 3$) to 0.00100 (-0.99 percent) (at $n = 11$), whereas P_F ranges from 0.00151 ($+49.51$ percent) (at $n = 3$) to 0.00102 ($+0.99$ percent) (at $n = 11$) using Method 5.

Method	Failure probability	Number of function evaluation[*]
Direct Monte Carlo simulation	0.00101	1,000,000
MPP(based univariate method (Rahman and Wei, 2006)	0.00101	167
First-order FHDMR	0.00102	49[**]
First-order HDMR	0.00161	49[**]
Second-order FHDMR	0.00101	1009[***]
Second-order HDMR	0.00102	1009[***]

Notes: [*]Total number of times the original performance function is calculated; [**]$(n - 1) \times N + 1 = (9 - 1) \times 6 + 1 = 49$; [***]$(n - 1)^2 (N - 1)N /2 + (n - 1)N + 1 = (9 - 1)^2(6 - 1)6/2 + (9 - 1)6 + 1 = 1009$
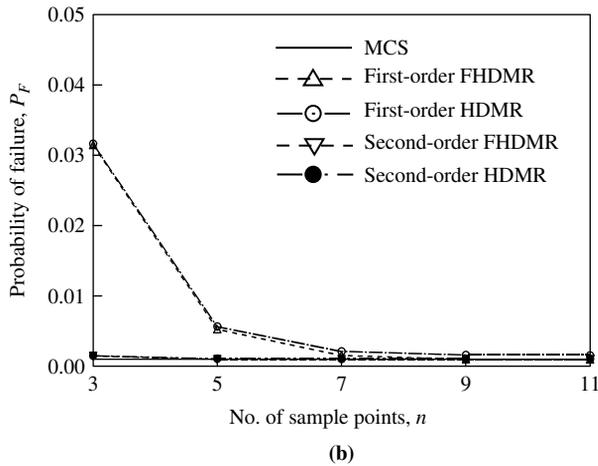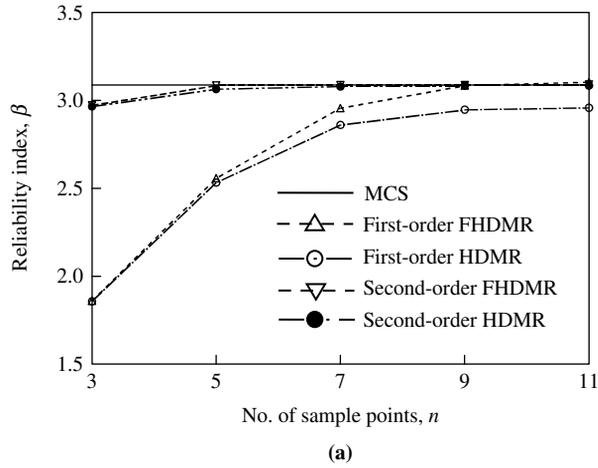
Compared with direct MCS, error in the estimated failure probability using different methods is tabulated in Table IX. It can be observed from Table IX that, Method 2 resulted in reduction of approximation error of the estimated failure probability from $+3.034 \times 10^3$ percent to $+3.016 \times 10^3$ percent for $n = 3$, from $+461.38$ percent to $+422.77$ percent for $n = 5$, from $+109.90$ percent to $+54.46$ percent for $n = 7$,

Method	Number of sample points, n				
	3	5	7	9	11
First-order FHDMR (percent)	$+3.02 \times 10^3$	$+422.77$	$+54.46$	$+0.99$	-4.95
First-order HDMR (percent)	$+3.03 \times 10^3$	$+461.38$	$+109.90$	$+59.41$	$+53.46$
Second-order FHDMR (percent)	$+46.53$	$+0.99$	0.00	0.00	$+0.99$
Second-order HDMR (percent)	$+49.51$	$+7.92$	$+2.97$	$+0.99$	$+0.99$

from $+59.41$ percent to $+0.99$ percent for $n = 9$, and from $+53.46$ to -4.95 percent for $n = 11$ compared with Method 3. Similarly, compared with Method 2, Method 4 resulted in drastic reduction of approximation error of the estimated failure probability from $+3.016 \times 10^3$ percent to $+46.53$ percent for $n = 3$, from $+422.77$ to $+0.99$ percent for $n = 5$, from $+54.46$ to 0.00 percent for $n = 7$, from $+0.99$ to 0.00 percent for $n = 9$, and from -4.95 to -0.99 percent for $n = 11$. Similar trend is observed by comparing the results obtained using Methods 3 and 4, by comparing the results obtained using Methods 3 and 5 and by comparing the results obtained using Methods 4 and 5. However, the computational effort in terms of number of function evaluations for second-order HDMR and FHDMR approximation (Methods 4 and 5) increased from 13 to 73 for $n = 3$, from 25 to 265 for $n = 5$, from 37 to 577 for $n = 7$, from 49 to 1009 for $n = 9$, and from 61 to 1561 for $n = 9$ when compared with first-order HDMR and FHDMR approximation (Methods 2 and 3).

Example 5. Fatigue crack growth of edge cracked plate

In this example, fatigue crack growth of an edge crack plate studied by Harkness *et al.* (1992), is considered. The objective of this example is to illustrate the effectiveness of the proposed method in solving fatigue reliability. Our analysis examines the uncertainty in fatigue life through characterization of the uncertainties in the parameters governing fatigue life and modeling crack growth.

Problem definition and input. Fatigue crack growth was modeled by the Paris law (Paris and Erdogan, 1963) in plane strain. According to this method, fatigue crack-initiation life N_F is defined as:

$$N_F \int_{a_i}^{a_f} \frac{\mathrm{d}a}{D(\Delta K_{eq})^{\eta}}, \tag{42}$$

where a_i is the initial crack length and a_f is the crack length at failure; D, η are the material parameters; ΔK_{eq} is the equivalent mode I stress intensity factor, K_I, at peak loading. According to Paris law crack growth occurs in the direction of maximum hoop stress and crack growth direction, θ, measured from the crack tip tangent, satisfies:

$$\sin \theta \, \Delta K_I + (3 \cos \theta - 1) \Delta K_{II} = 0, \tag{43}$$

and ΔK_{eq} is:

$$\Delta K_{eq} = \cos^2(\theta/2)[\cos(\theta/2)\Delta K_I - 3 \sin(\theta/2)K_{II}], \tag{44}$$

Failure is defined as the fatigue life N_F, is less than the design threshold value, N_I. The design threshold value is based on target reliability and therefore, can be controlled. It can be observed from equation (42) that fatigue life expression involves several uncertain variables, making the fatigue life uncertain. The limit state/performance function can be expressed as:

$$g(x) = N_F(x) - N_I. \tag{45}$$

Since negative and very small positive values of growth parameters D and η are unrealistic, therefore, shifted log-normal distributions are assigned to both parameters. The statistical parameters and the marginal densities of the random variables are presented in Table X. For evaluating the failure probability P_F, seven equally spaced

sample points ($n = 7$) are deployed along each of the variable axis to form first-order approximation of the function in equation (45). The reference point is taken as the mean values of the random variables. Figure 13 compares the variation of failure probability with design threshold value obtained by different methods. It can be observed that, Method 2 provides significant accuracy to the failure probability estimation, when compared with direct MCS results, while using Method 3 large amount of error is accumulated in the predicted result. Accumulation of the large amount of error using Method 3 can be attributed to neglecting the higher order cooperative effects in Method 3 and multiplicative nature of the limit state/performance function. However, both Methods 2 and 3 needs only 37 function evaluations, while direct MCS requires $10^5 - 10^9$ number of original function evaluations, respectively, for different design threshold values.

Seven equally spaced sample points ($n = 7$) along each of the variable axis is selected to form a regular grid, for second-order approximation using Methods 4 and 5. The reference point is taken as the mean values of the random variables. Figure 13 also presents the variation of the failure probability P_F with design threshold value using

Random variable	Mean	Cov	Distribution type
D	6.8×10^{-12}	0.05	Lognormal
n	3.60	0.01	Lognormal
σ_{max}	75	0.03	Gaussian
σ_{min}	25	0.03	Gaussian
a_i	3.1×10^{-4}	0.186	Uniform*
K_{IC}	165	0.015	Lognormal

Note: *Uniformly distributed over ($2.1 \times 10^{-4} - 4.1 \times 10^{-4}$)

Table X.
Statistical properties of the random variables for Example 5
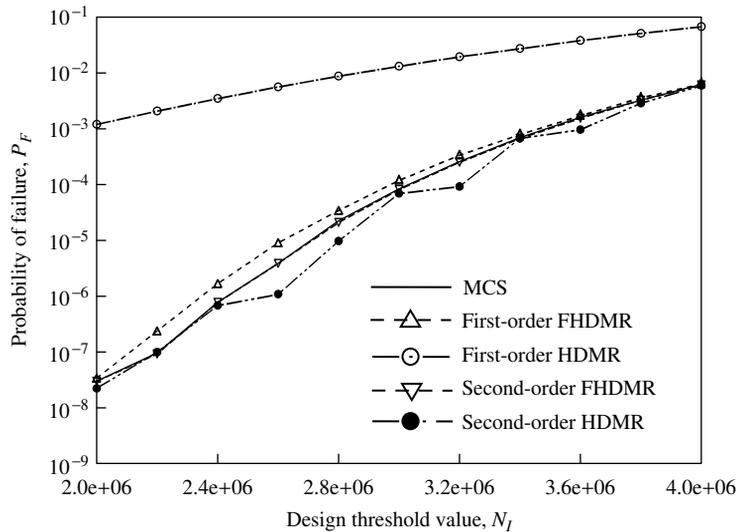
Figure 13.
Variation of failure probability (Example 5)

Methods 4 and 5. It can be observed from Figure 13 that Method 4 almost exactly estimate the failure probability compared to the benchmark results obtained using Method 1. In addition, the results obtained using Method 5, are closely matching with the direct MCS. This is attributed due to consideration of the second-order cooperative effects in approximations using Method 5. But the number of function evaluations required using Methods 4 and 5 are 577 compared with 37 function evaluations for Methods 2 and 3. Therefore, to make a balance between the computational cost in terms of function evaluations and the accuracy, Method 2 seems most suitable, especially for multiplicative nature of the limit state/performance function.

The effect of number of sample points used for first and second-order approximation on the reliability estimation is examined by carrying a similar analysis varying n form 3 to 9. Figure 14 (a) and (b) presents, respectively, the variation
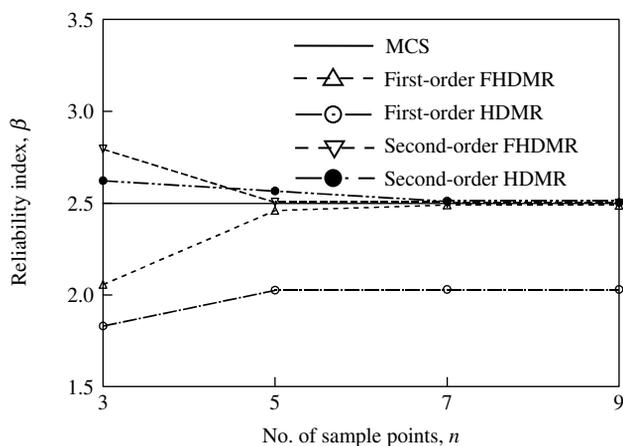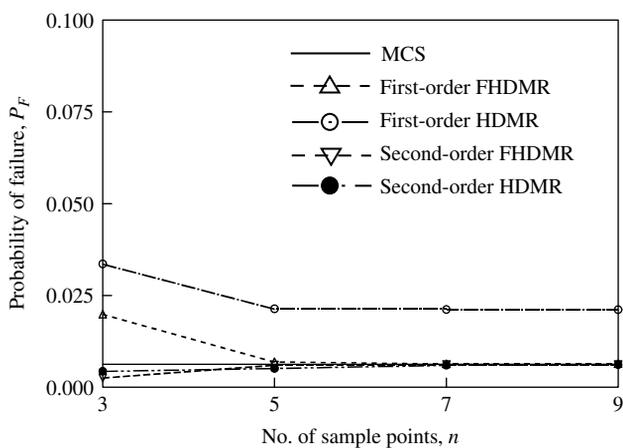

Figure 14.
Variation of reliability estimation (Example 5).
(a) Reliability index, β;
(b) probability of failure, P_F

of the reliability index β and the estimated failure probability P_F with respect to number of sample points, for design threshold value, $N_I = 4 \times 10^6$. It can be observed from Figure 14 that very small value of n gives rise to large error due to lose of uncertainty information in approximation of the limit state/performance function using Methods 2 and 4. Similar trend is also found by comparing the results obtained using Methods 3 and 5. However, the computational effort in terms of number of function evaluations for second-order HDMR and FHDMR (Methods 4 and 5) increased from 13 to 73 for $n = 3$, from 25 to 265 for $n = 5$, from 37 to 577 for $n = 7$, from 49 to 1009 for $n = 9$, and from 61 to 1561 for $n = 9$ when compared with first-order HDMR and FHDMR approximation (Methods 2 and 3).

Summary and conclusions

This paper addressed a comparative assessment of approximation methods based on HDMR and FHDMR for predicting the failure probability of systems subject to random loads, material properties, and geometry in an efficient manner. Five numerical examples are illustrated to show the performance of approximation techniques based on first- and second-order HDMR/FHDMR. Comparisons were made with direct MCS to evaluate the accuracy and computational efficiency of the present methods. HDMR approximation works well when the sought multivariate response function has an additive nature. This is because of the structure of the right hand side of HDMR expansion. But, for multiplicative nature of the multivariate response function, HDMR based method cannot be useful. At this juncture, the factorized form of HDMR can be used for approximation of an implicit limit state/performance function. This method works superior when the response function is dominantly of multiplicative nature. However, inclusion of the higher order cooperative effects in HDMR approximation provides significant accuracy to the limit state/performance function of dominantly multiplicative nature, but the number of original function evaluation increases significantly over first-order HDMR/FHDMR approximation. Numerical examples also support these observations. It is observed that HDMR/FHDMR based approximation methods not only yields more accurate estimate of the probability of failure than the alternative approximate methods in highly nonlinear problems, but also reduces the computational effort significantly over direct simulation method.

A parametric study on HDMR and FHDMR approximation methods has also been reported in this paper. First-order FHDMR approximation provides desired accuracy to the predicted failure probability with least number of function evaluations. In order to reduce the approximation error further, second-order FHDMR approximation could be used in reliability analysis, but the number of function evaluations increases significantly compared to first-order. Number of sample points n used in first and second-order approximation was set to different values to investigate its effect on the estimated failure probability. Very small value of n should be avoided owing to lose of uncertainty information in present approximation methods.

References

Alis, O.F. and Rabitz, H. (2001), "Efficient implementation of high dimensional model representations", *Journal of Mathematical Chemistry*, Vol. 29 No. 2, pp. 127-42.

Ang, A.H.S. and Tang, W.H. (1975), *Probability Concepts in Engineering Planning and Design, Basic Principles*, Vol. 1, Wiley, New York, NY.

Au, S.K. and Beck, J.L. (2001), "Estimation of small failure probabilities in high dimensions by subset simulation", *Probabilistic Engineering Mechanics*, Vol. 16 No. 4, pp. 263-77.

Bjerager, P. (1988), "Probability integration by directional simulation", *Journal of Engineering Mechanics, ASCE*, Vol. 14 No. 8, pp. 285-1302.

Breitung, K. (1984), "Asymptotic approximations for multinormal integrals", *Journal of Engineering Mechanics, ASCE*, Vol. 110 No. 3, pp. 357-66.

Chowdhury, R., Rao, B.N. and Prasad, A.M. (2007), "High dimensional model representation for piece wise continuous function approximation", *Communications in Numerical Methods in Engineering*.

Chowdhury, R., Rao, B.N. and Prasad, A.M. (2008), "High dimensional model representation for structural reliability analysis", *Communications in Numerical Methods in Engineering*, Vol. 25 Nos 7/8.

Der Kiureghian, A. and Dakessian, T. (1998), "Multiple design points in first and second-order reliability", *Structural Safety*, Vol. 20 No. 1, pp. 37-49.

Ditlevsen, O. and Madsen, H.O. (1996), *Structural Reliability Methods*, Wiley, Chichester.

Harkness, H.H., Belytschko, T.D. and Liu, W.K. (1992), "Finite element reliability analysis of fatigue life", *Nuclear Engineering and Design*, Vol. 133, pp. 209-24.

Lancaster, P. and Salkauskas, K. (1986), *Curve and Surface Fitting: An Introduction*, Academic Press, London.

Li, G., Rosenthal, C. and Rabitz, H. (2001a), "High dimensional model representations", *Journal of Physical Chemistry A*, Vol. 105, pp. 7765-77.

Li, G., Wang, S.W. and Rabitz, H. (2001b), "High dimensional model representations generated from low dimensional data samples − I. mp − Cut-HDMR", *Journal of Mathematical Chemistry*, Vol. 30 No. 1, pp. 1-30.

Li, G., Wang, S.W., Rabitz, H., Wang, S. and Jaffé, P. (2002), "Global uncertainty assessments by high dimensional model representations (HDMR)", *Chemical Engineering Science*, Vol. 57 No. 21, pp. 4445-60.

Liu, P.L. and Der Kiureghian, A. (1991), "Finite element reliability of geometrically nonlinear uncertain structures", *Journal of Engineering Mechanics, ASCE*, Vol. 117 No. 8, pp. 1806-25.

Madsen, H.O., Krenk, S. and Lind, N.C. (1986), *Methods of Structural Safety*, Prentice-Hall, Englewood Cliffs, NJ.

Melchers, R.E. (1989), "Importance sampling in structural systems", *Structural Safety*, Vol. 6 No. 1, pp. 3-10.

Paris, P.C. and Erdogan, F. (1963), "A critical analysis of crack propagation laws", *Journal of Basic Engineering, ASME*, Vol. 85, pp. 528-34.

Rabitz, H. and Alis, O.F. (1999), "General foundations of high dimensional model representations", *Journal of Mathematical Chemistry*, Vol. 25 Nos 2/3, pp. 197-233.

Rabitz, H., Alis, O.F., Shorter, J. and Shim, K. (1999), "Efficient input-output model representations", *Computer Physics Communications*, Vol. 117 Nos 1/2, pp. 11-20.

Rackwitz, R. (2001), "Reliability analysis – a review and some perspectives", *Structural Safety*, Vol. 23 No. 4, pp. 365-95.

Rahman, S. and Wei, S. (2006), "A univariate approximation at most probable point for higher-order reliability analysis", *International Journal of Solids and Structures*, Vol. 43, pp. 2820-39.

Rao, B.N. and Rahman, S. (2000), "An efficient meshless method for fracture analysis of cracks", *Computational Mechanics*, Vol. 26, pp. 398-408.

Rubinstein, R.Y. (1981), *Simulation and the Monte Carlo Method*, Wiley, New York, NY.

Schuëller, G.I., Pradlwarter, H.W. and Koutsourelakis, P.S. (2004), "A critical appraisal of reliability estimation procedures for high dimensions", *Probabilistic Engineering Mechanics*, Vol. 19 No. 4, pp. 463-74.

Shan, S. and Wang, G.G. (2006), "Failure surface frontier for reliability assessment on expensive performance function, ASME Transactions", *Journal of Mechanical Design*, Vol. 128, pp. 1227-35.

Singh, I.V. (2004), "A numerical solution of composite heat transfer problems using meshless method", *International Journal of Heat and Mass Transfer*, Vol. 47, pp. 2123-38.

Sobol, I.M. (2003), "Theorems and examples on high dimensional model representations", *Reliability Engineering & System Safety*, Vol. 79 No. 2, pp. 187-93.

Tunga, M.A. and Demiralp, M. (2004), "A factorized high dimensional model representation on the partitioned random discrete data", *Applied Numerical Analysis and Computational Mathematics*, Vol. 1 No. 1, pp. 231-41.

Tunga, M.A. and Demiralp, M. (2005), "A factorized high dimensional model representation on the nods of a finite hyperprismatic regular grid", *Applied Mathematics and Computation*, Vol. 164, pp. 865-83.

Wang, S.W., Levy, H. II, Li, G. and Rabitz, H. (1999), "Fully equivalent operational models for atmospheric chemical kinetics within global chemistry-transport models", *Journal of Geophysical Research*, Vol. 104, D23, pp. 30417-26.

Further reading

ADINA R&D, Inc. (2005), "ADINA theory and modeling guide", Report ARD 05-6.

Corresponding author

B.N. Rao can be contacted at: bnrao@iitm.ac.in

This article has been cited by:

1. Wenliang Fan, Jinghong Wei, Alfredo H-S Ang, Zhengliang Li. 2016. Adaptive estimation of statistical moments of the responses of random systems. *Probabilistic Engineering Mechanics* **43**, 50-67. [CrossRef]

2. Xiaoke Li, Haobo Qiu, Zhenzhong Chen, Liang Gao, Xinyu Shao. 2015. A local sampling method with variable radius for RBDO using Kriging. *Engineering Computations* **32**:7, 1908-1933. [Abstract] [Full Text] [PDF]

3. Burcu Tunga, Metin Demiralp. 2012. A novel approximation method for multivariate data partitioning. *Engineering Computations* **29**:7, 743-765. [Abstract] [Full Text] [PDF]

4. R. Chowdhury, S. Adhikari. 2012. Fuzzy parametric uncertainty analysis of linear dynamical systems: A surrogate modeling approach. *Mechanical Systems and Signal Processing* **32**, 5-17. [CrossRef]

5. Jorge E. Hurtado, Diego A. Alvarez. 2012. The encounter of interval and probabilistic approaches to structural reliability at the design point. *Computer Methods in Applied Mechanics and Engineering* **225-228**, 74-94. [CrossRef]

6. R. Chowdhury, S. Adhikari. 2011. Reliability analysis of uncertain dynamical systems using correlated function expansion. *International Journal of Mechanical Sciences* **53**, 281-285. [CrossRef]

7. S. Adhikari, R. Chowdhury, M.I. Friswell. 2011. High dimensional model representation method for fuzzy structural dynamics. *Journal of Sound and Vibration* **330**, 1516-1529. [CrossRef]

8. Rajib Chowdhury, B.N. Rao. 2010. Probabilistic stability assessment of slopes using high dimensional model representation. *Computers and Geotechnics* **37**, 876-884. [CrossRef]

9. B.N. Rao, Rajib Chowdhury, A. Meher Prasad, R.K. Singh, H.S. Kushwaha. 2010. Reliability analysis of 500MWe PHWR inner containment using high-dimensional model representation. *International Journal of Pressure Vessels and Piping* **87**, 230-238. [CrossRef]

10. Burcu Tunga, Metin Demiralp. 2009. Constancy maximization based weight optimization in high dimensional model representation. *Numerical Algorithms* **52**, 435-459. [CrossRef]